Science Immunology
AAAS

Supplementary Materials for

Salmonella Typhi Vi capsule prime-boost vaccination induces convergent and functional antibody responses

Lindsay C. Dahora *et al.*

Corresponding author: Lindsay C. Dahora, lcd26@duke.edu; Georgia D. Tomaras, gdt@duke.edu

Sci. Immunol. **6**, eabj1181 (2021)
DOI: 10.1126/sciimmunol.abj1181

The PDF file includes:

Figs. S1 to S13

Other Supplementary Material for this manuscript includes the following:

Data S1 to S3

Supplementary Materials

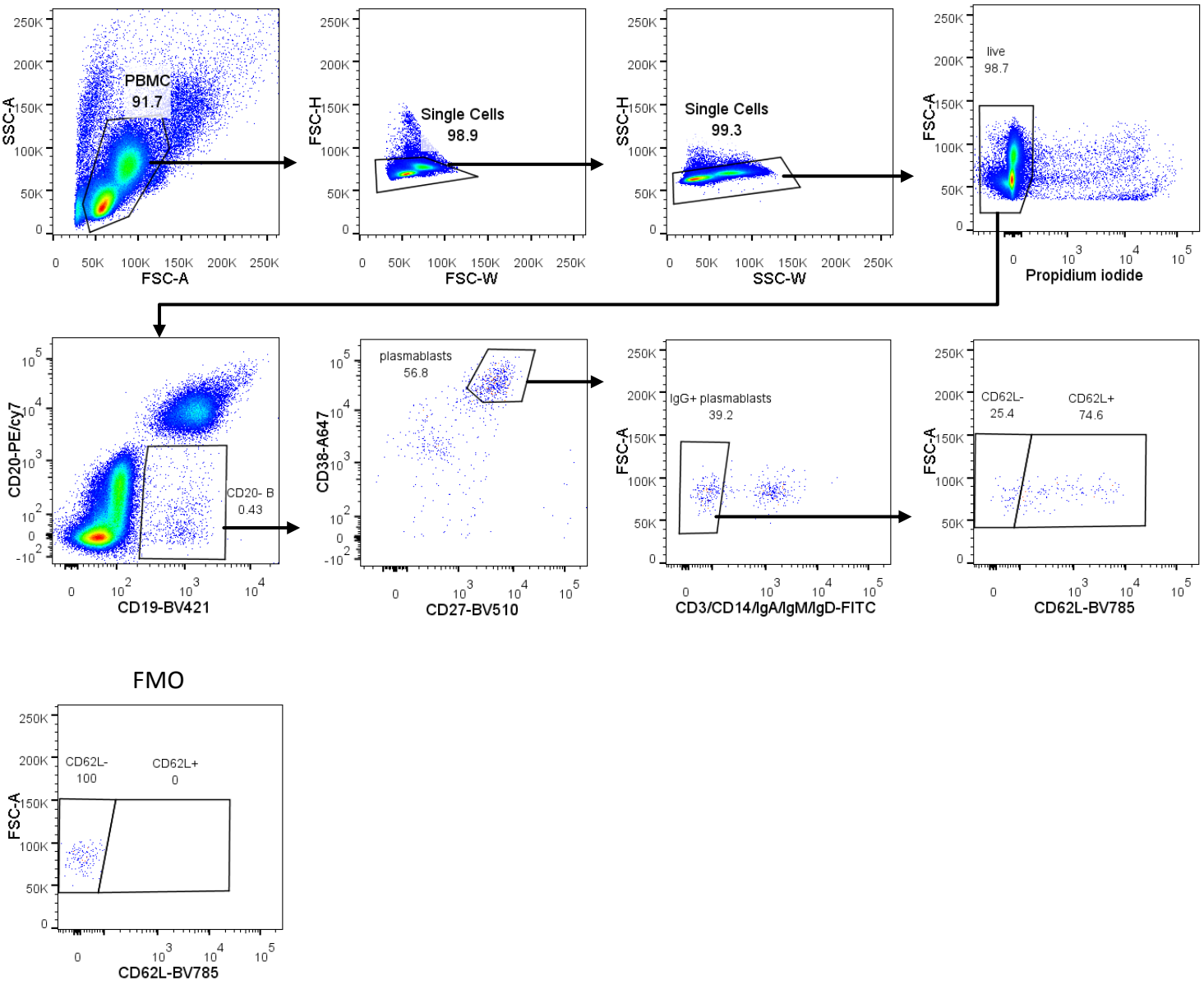

FMO

Fig. S1 – Example gating strategy for sorting of IgG$^+$ plasmablasts from human vaccinee PBMCs

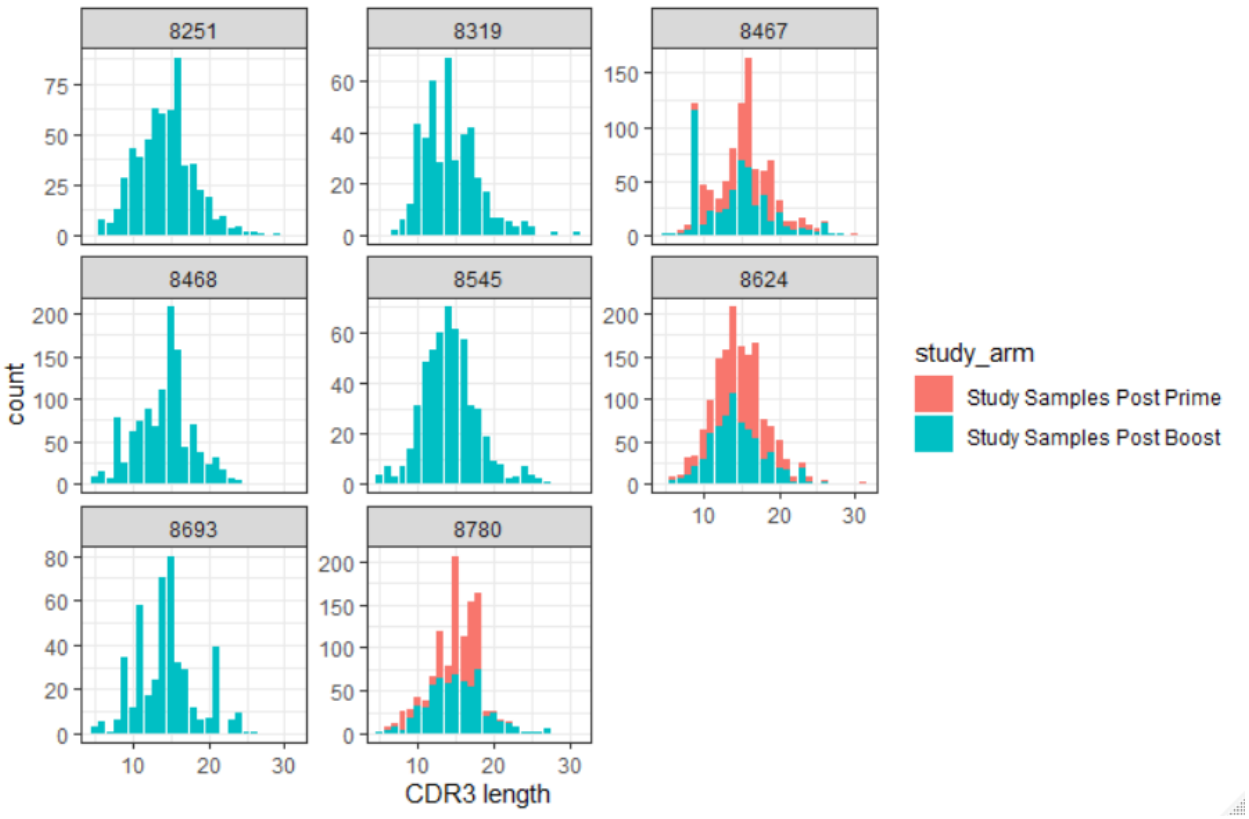

Fig. S2 – Heavy chain CDR3 length after Vi-TT primary immunization or Vi-PS-boost immunization

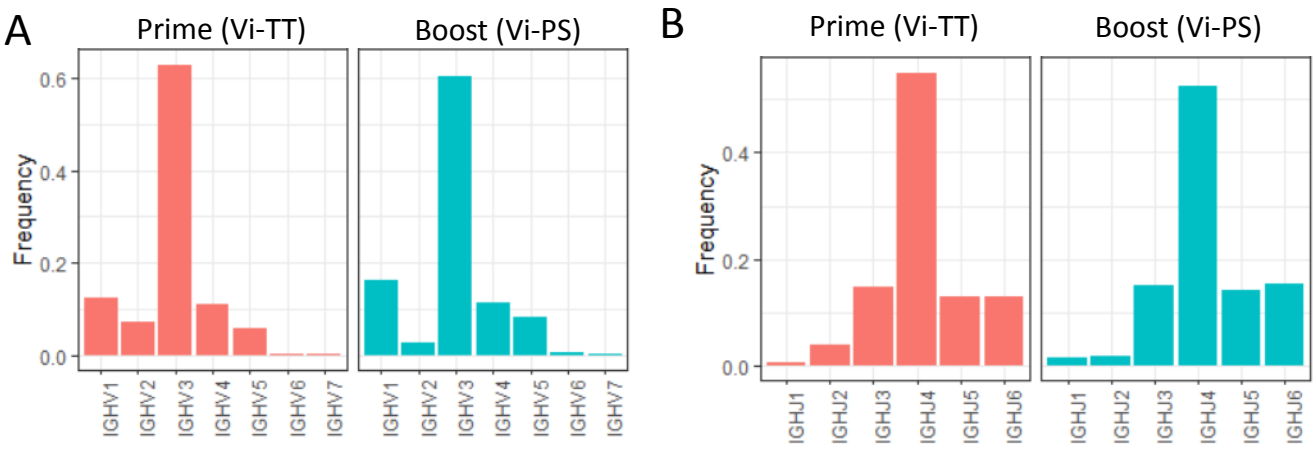

Fig. S3 – Sequence characteristics of BCRs from IgG-positive plasmablasts after Vi-TT primary or Vi-PS boost immunization

A) Ig heavy chain variable region usage, showing samples that were paired between immunization (n=3). B) Ig heavy chain junction region usage, showing samples that were paired between immunizations (n=3).

Fig. S4 – Sequence characteristics of BCRs from IgG-positive plasmablasts after Vi-TT primary or Vi-PS boost immunization, focusing on Ig heavy chain variable regions
Ig heavy chain variable region usage, showing the usage after the Vi-TT prime and Vi-PS boost immunizations for the 3 individuals for who data after both vaccines was available.

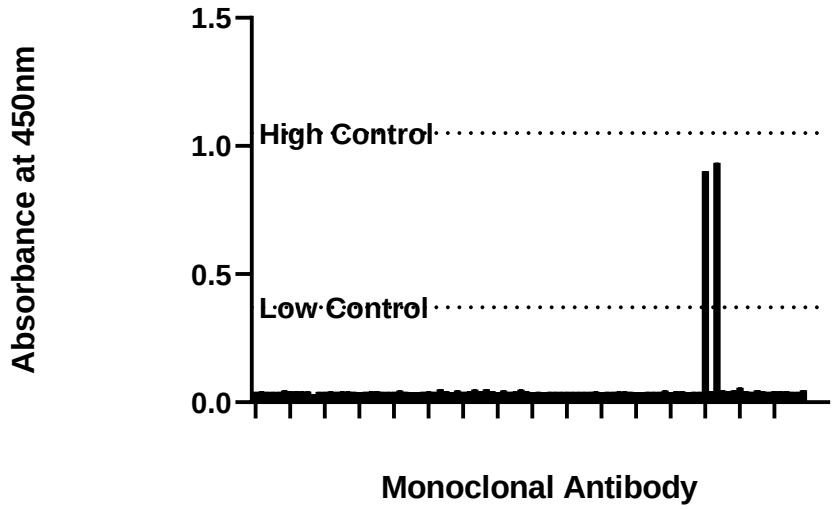

Fig. S5 – Monoclonal antibody binding to tetanus toxoid
Antibody binding was measured using the VaccZyme TetanusToxoid ELISA. The monoclonal antibodies were added to the plate at a concentration of 100 ng/ml. Two monoclonal antibodies were shown to bind tetanus toxoid. The positive antibodies are AB-007975 and AB-007990. Both of these were negative for Vi antigen binding in the Vi polysaccharide ELISA.

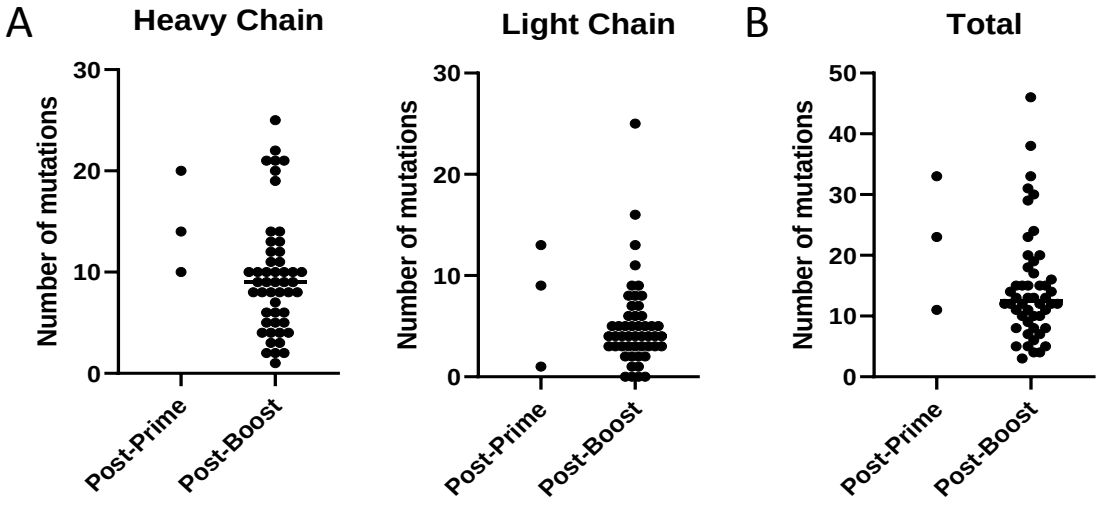

Fig. S6 – Somatic hypermutations in sequences of Vi-positive monoclonal antibodies
A) Number of somatic hypermutations in V heavy and V light chain after either primary immunization with Vi-TT (n=3) or after a boost with Vi-PS (n=50). B) Total number of somatic hypermutations in both chains after prime and boost. The number of mutations shown contains both silent and non-silent mutations. The horizontal line indicates the median.

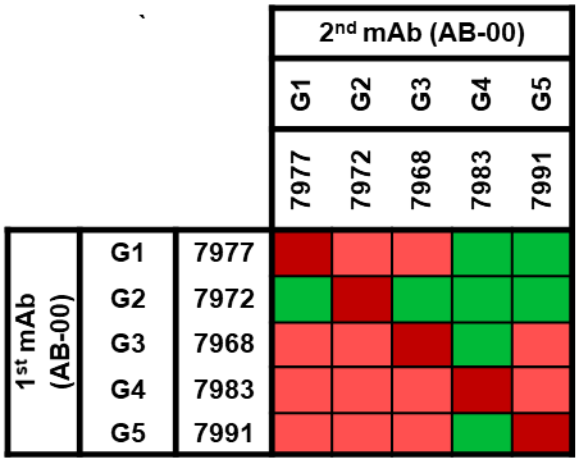

Fig. S7 – Antibodies across different families have similar epitope specificities
Cross-competition between representative mAbs from each convergent family where ViPS antigen is immobilized at low density on biosensor, following by saturated binding of 1st mAb, followed by binding of 2nd mAb. Red indicates self-blocking, pink indicates cross-blocking, and green indicates no blocking.

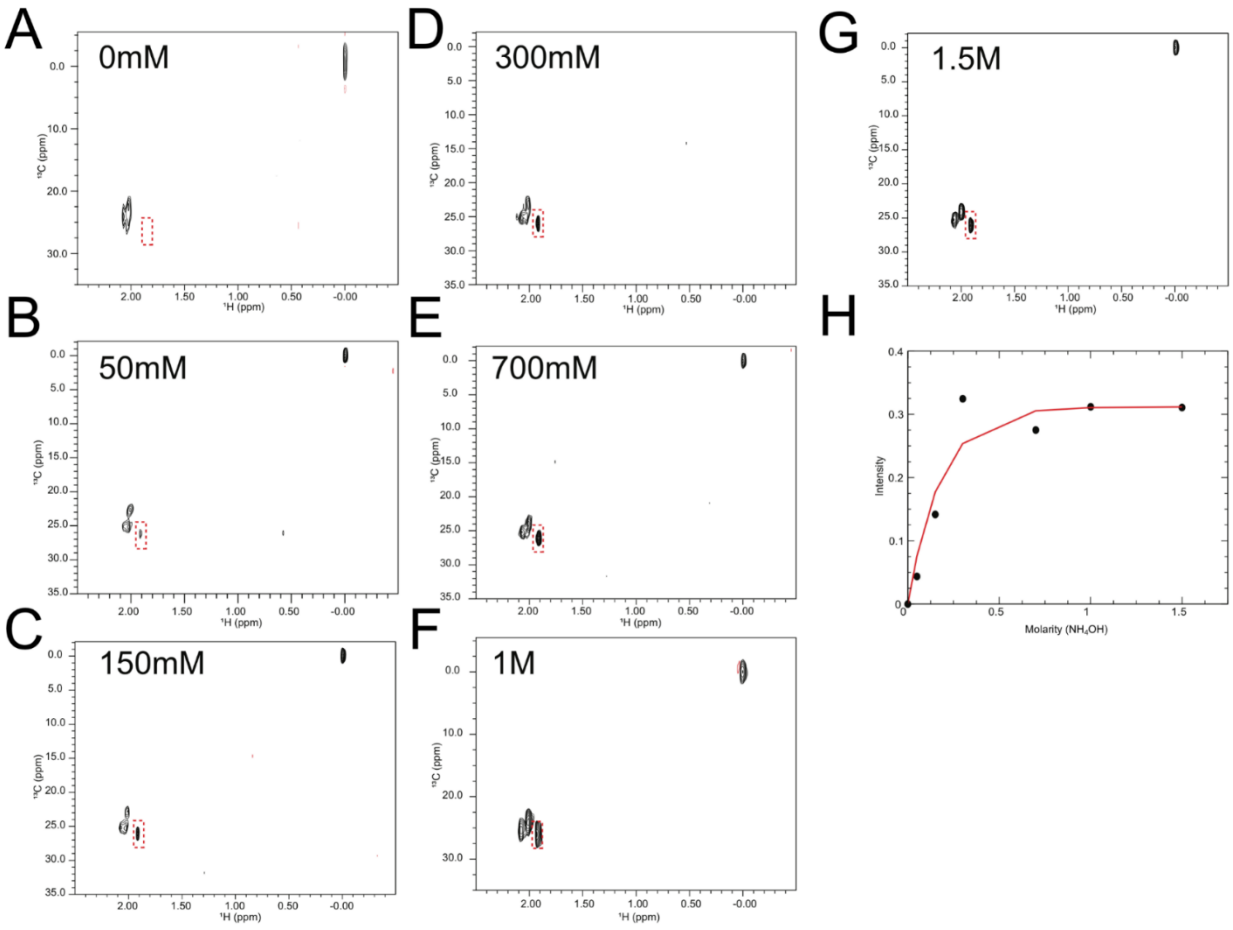

Fig. S8 – Full ^{1}H–^{13}C HSQC NMR analysis of Vi polysaccharide solutions as function of increasing NH_4OH treatment

2D NMR spectra of (A) untreated, (B) 0.05 M NH_4OH-treated, (C) 0.15 M NH_4OH-treated, (D) 0.3 M NH_4OH-treated, (E) 0.7 M NH_4OH-treated, (F) 1 M NH_4OH-treated, and (G) 1.5 M NH_4OH-treated *C. freundii* Vi solutions. The x- and y- axis contain the NMR resonances arising from ^{1}H and ^{13}C, respectively, representing ^{1}H-^{13}C direct bonds. Panel H represents the increasing signal (centered around 1.9 ppm (^{1}H) and 26.5 ppm (^{13}C) – dotted red box in each panel) as function of increasing amounts of NH_4OH treatment.

A

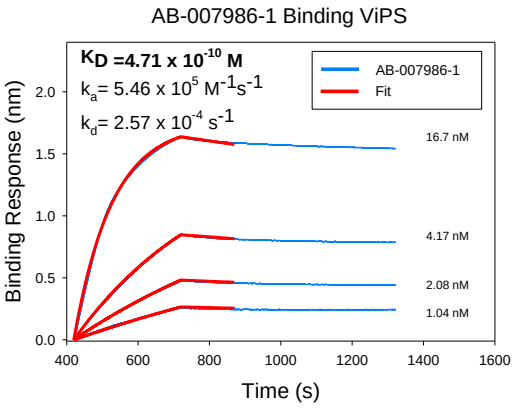
AB-007986-1 Binding ViPS
K_D =4.71 x 10^{-10} M
k_a= 5.46 x 10^5 $M^{-1}s^{-1}$
k_d= 2.57 x 10^{-4} s^{-1}
AB-007986-1
Fit
16.7 nM
4.17 nM
2.08 nM
1.04 nM
Binding Response (nm)
Time (s)

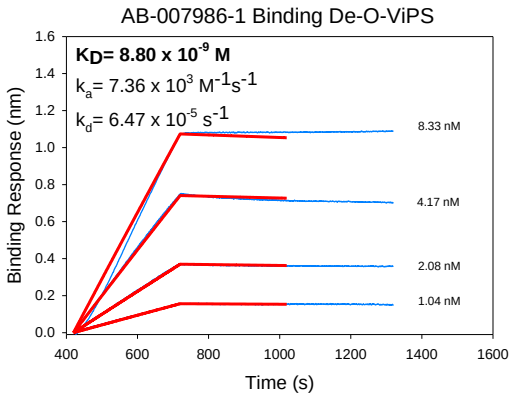
AB-007986-1 Binding De-O-ViPS
K_D= 8.80 x 10^{-9} M
k_a= 7.36 x 10^3 $M^{-1}s^{-1}$
k_d= 6.47 x 10^{-5} s^{-1}
8.33 nM
4.17 nM
2.08 nM
1.04 nM
Binding Response (nm)
Time (s)

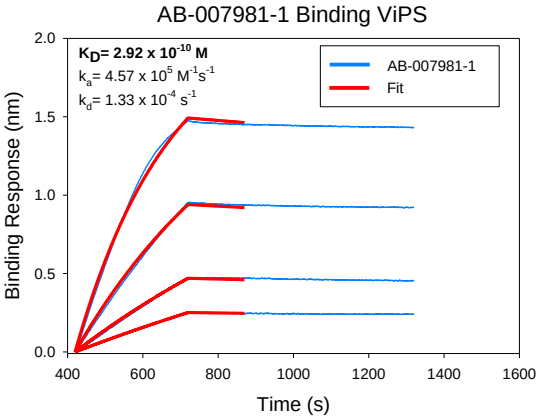
AB-007981-1 Binding ViPS
K_D= 2.92 x 10^{-10} M
k_a= 4.57 x 10^5 $M^{-1}s^{-1}$
k_d= 1.33 x 10^{-4} s^{-1}
AB-007981-1
Fit
Binding Response (nm)
Time (s)

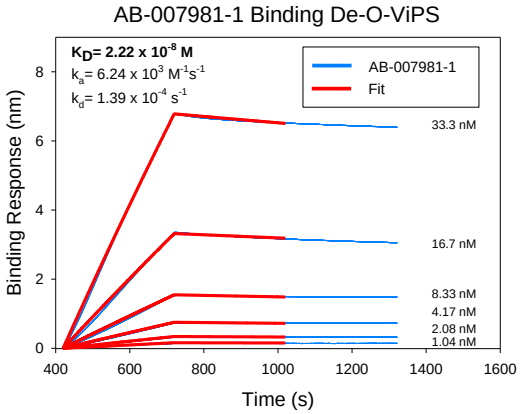
AB-007981-1 Binding De-O-ViPS
K_D= 2.22 x 10^{-8} M
k_a= 6.24 x 10^3 $M^{-1}s^{-1}$
k_d= 1.39 x 10^{-4} s^{-1}
AB-007981-1
Fit
33.3 nM
16.7 nM
8.33 nM
4.17 nM
2.08 nM
1.04 nM
Binding Response (nm)
Time (s)

B

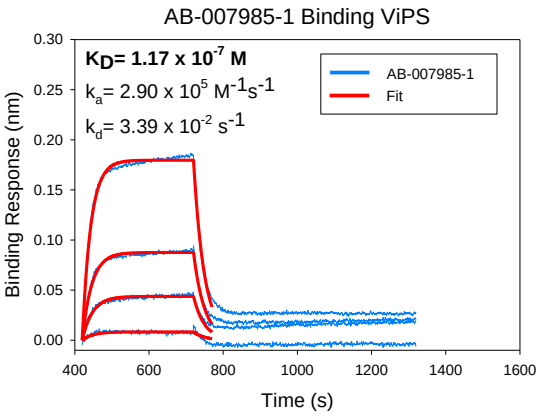
AB-007985-1 Binding ViPS
K_D= 1.17 x 10^{-7} M
k_a= 2.90 x 10^5 $M^{-1}s^{-1}$
k_d= 3.39 x 10^{-2} s^{-1}
AB-007985-1
Fit
Binding Response (nm)
Time (s)

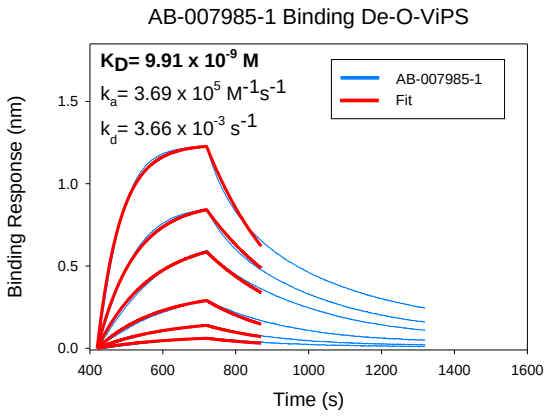
AB-007985-1 Binding De-O-ViPS
K_D= 9.91 x 10^{-9} M
k_a= 3.69 x 10^5 $M^{-1}s^{-1}$
k_d= 3.66 x 10^{-3} s^{-1}
AB-007985-1
Fit
Binding Response (nm)
Time (s)

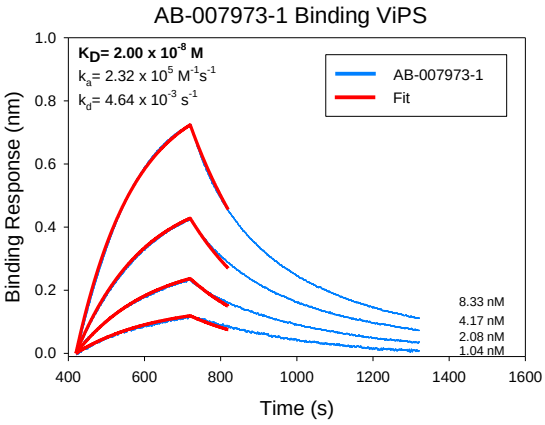
AB-007973-1 Binding ViPS
K_D= 2.00 x 10^{-8} M
k_a= 2.32 x 10^5 $M^{-1}s^{-1}$
k_d= 4.64 x 10^{-3} s^{-1}
AB-007973-1
Fit
8.33 nM
4.17 nM
2.08 nM
1.04 nM
Binding Response (nm)
Time (s)

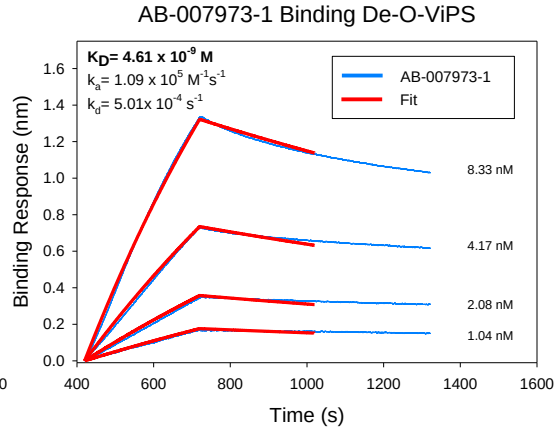
AB-007973-1 Binding De-O-ViPS
K_D= 4.61 x 10^{-9} M
k_a= 1.09 x 10^5 $M^{-1}s^{-1}$
k_d= 5.01x 10^{-4} s^{-1}
AB-007973-1
Fit
8.33 nM
4.17 nM
2.08 nM
1.04 nM
Binding Response (nm)
Time (s)

Fig. S9 – Monoclonal antibodies derived by vaccination target non-*O*-acetylated Vi
A) Binding sensorgrams of monoclonal antibodies that bind with similar avidity to Vi polysaccharide (left) and de-O-acetylated Vi polysaccharide (right) with corresponding avidity measurements indicated. B) Binding sensorgrams of monoclonal antibodies that bind with weaker avidity to Vi polysaccharide (left) compared to de-O-acetylated Vi polysaccharide (right) with corresponding avidity measurements indicated.

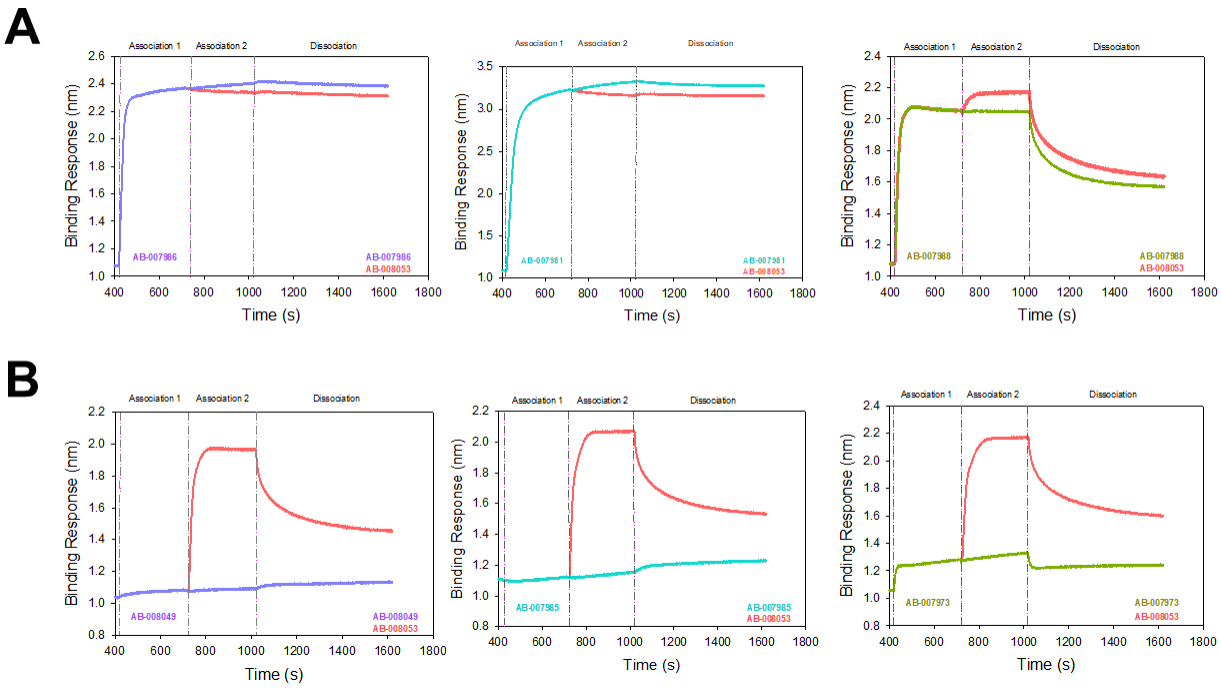

Fig. S10 – ViPS monoclonal antibodies recognize exposed and occluded epitopes
Competition experiments performed by immobilizing low level ViPS antigen to biosensor, dipping into antibody 1 until binding is completely saturated, and then dipping into antibody 2. A) Competition of SEE mAbs in reverse orientation with SEE mAbs as antibody 1 and AB-008053 as antibody 2. B) Competition of SEO mAbs in reverse orientation with SEO mAbs as antibody 1 and AB-008053 as antibody 2.

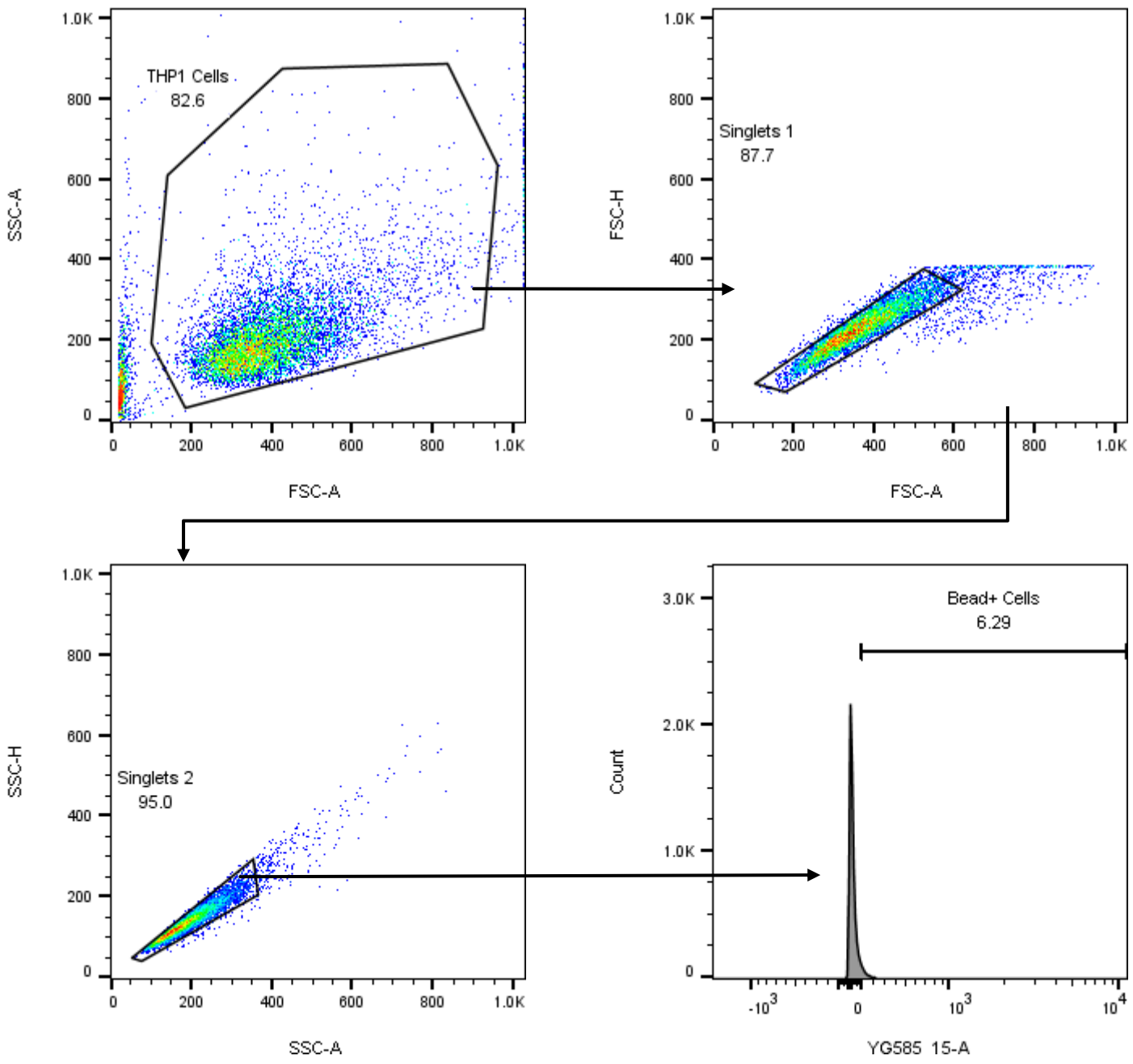

Fig. S11 – Example of the ADMP gating strategy
Initially, single cells are gated, followed by a selection of bead-positive cells. The gate for the bead-positive cells is based on a negative control THP-1 sample without any beads. Both the percentage of bead-positive cells and the intensity of the beads are used to calculate the phagocytic score.

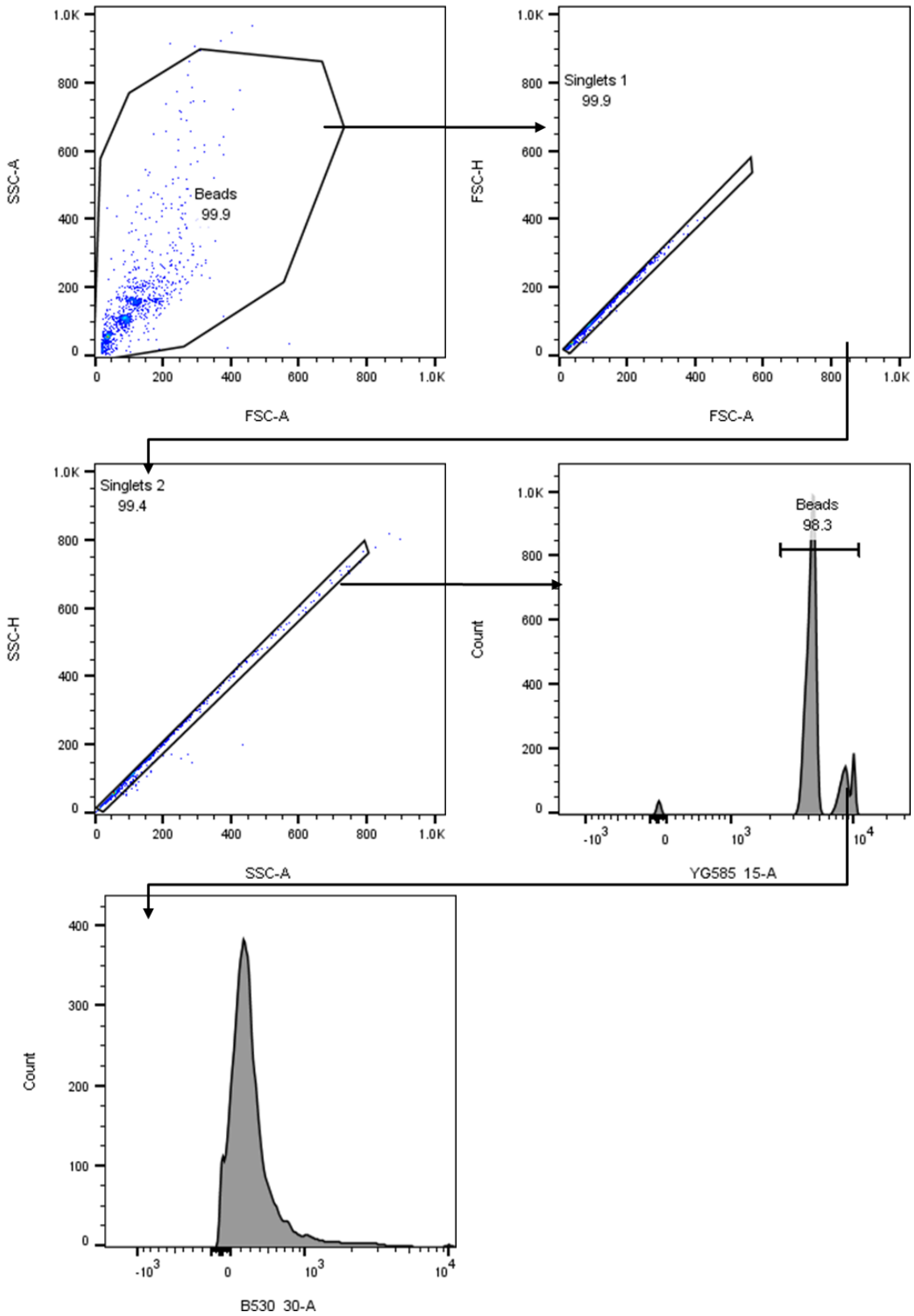

Fig. S12 – Example of the ADCD gating strategy
Initially, single beads are gated, after which the anti-guinea pig C3-FITC intensity is measured using geometric mean fluorescent intensity.

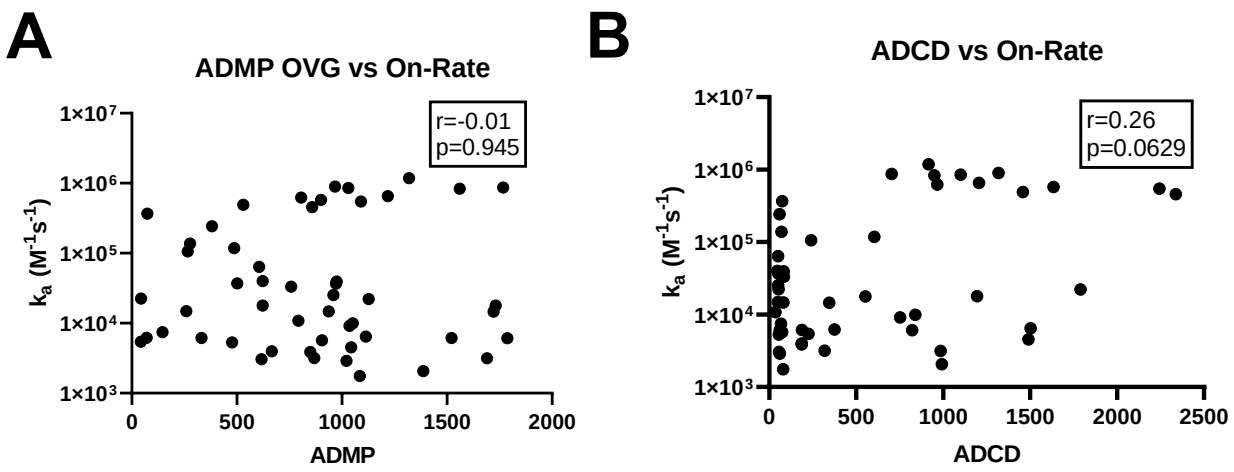

Fig. S13 – ADMP and ADCD potential are not associated with antibody on-rate
Spearman correlations of A) ADMP score and Vi on-rate. B) ADCD score and Vi on-rate.